INSPECTION AND REHABILITATION OF FIRE-DAMAGED REINFORCED CONCRETE STRUCTURES

ANA SOFIA TORRES BORGES VIEIRA INSTITUTO SUPERIOR TÉCNICO

OCTOBER 2017

Abstract

Reinforced concrete (RC) structures present in general a good fire behaviour, due to the non-combustibility of the constituent materials and the relatively low thermal conductivity of concrete. However, RC structures can suffer fire-induced damage, depending on the severity of the fire. As a result of the exposure to very high temperatures during a fire, the mechanical properties of concrete and reinforcing steel bars may be significantly reduced, which lead to a loss of strength of the RC structures. RC slabs are especially prone to be damaged by fire due to their lower thickness and concrete cover. Thus, it is important to define the residual mechanical properties of concrete and steel through inspection tests in order to design appropriate repair solutions. The main goal of the present study was to assess both field and laboratory inspection techniques applied to fire-damaged RC slabs and then investigate the bending behaviour of fire-damaged RC slabs repaired and strengthened with near surface mounted (NSM) carbon fibre reinforced polymers (CFRP) strips. To this end, an experimental program was performed, which consisted in subjecting simply supported RC slabs to the ISO 834 standard fire curve and a service mechanical load. In order to study two different deterioration levels, the slabs were exposed to fire for 60 and 120 minutes. Different concrete inspection tests were performed (visual assessment, ultrasonic pulse velocity test, Schmidt test, and Fire Behavior Test – FBTest, comprising splitting tensile tests and water absorption tests) and tensile tests were also performed on steel rebars. In addition, an unheated slab, and two fire-damaged slabs, one unrepaired and the other CFRP-strengthened, were subjected to flexural tests at room temperature, with the aim of measuring (i) the effect of the fire-damage and of (ii) the efficacy of the NSM-CFRP strips, respectively. The results obtained show that in general the *in situ* inspection tests presented a very significant scatter. The application of the UPV and *Schmidt* tests at different depths did not provide reliable results, confirming that these methods do not provide sufficiently accurate results (*i.e*. representative of the actual damage underwent by concrete) when applied to concrete samples of reduced size. It was found that the splitting tensile test (carried out within the FBTest) provided more conclusive results about the degradation of the concrete properties subjected to elevated temperatures compared to the water absorption test. The load capacity of the slab repaired with NSM CFRP strips was considerably improved, although it was not possible to explore the ductility of the steel rebars.

Keywords: reinforced concrete, fire exposure, inspection tests, repair techniques, CFRP strips, experimental study.

1. Introduction

The increasing use of RC at the beginning of the 20th century was due to the several advantages of this material when compared with other building materials used at that time (e.g. wood, masonry), namely its high compressive strength and reduced costs. In addition, RC structures present in general a good fire behaviour (especially when compared to steel structures), due to the relatively low thermal conductivity of concrete and the non-combustibility of the constituent materials, which do not produce smoke or toxic gases. Nevertheless, the physical, chemical and mechanical properties of concrete and steel rebars may be negatively affected when subjected to fire, which lead to a loss of strength of the RC structures [1]. A proper assessment of an RC structure after a fire event involves both field and laboratory work to determine the extent of fire-induced damage, as well as the residual properties of concrete and reinforcing steel bars, in order to design appropriate and cost effective repairs. RC slabs are especially prone to fire damage due to their lower thickness and concrete cover – the present study is focused on these RC structural elements.

Visual inspection can be considered as the main on-site technique, and it is used to classify the degree of damage for each structural concrete member; it includes the observation of colour changes, deflection, cracking, surface crazing, spalling or collapse of structural RC members [2].

Ultrasonic pulse velocity (UPV) is a non-destructive technique that can be used to estimate the concrete strength degradation after exposure to elevated temperatures. The principle of UPV measurements involves sending a pulse wave through a concrete sample/member, measuring the travel time and finally computing the corresponding velocity; higher UPVs correspond to higher compactness/uniformity (less cracks and voids) and, consequently, higher strength [3]. Yang *et al.* [4] performed an experimental investigation on concrete specimens heated in an electric furnace up to temperatures ranging from 400 ºC to 600 ºC, and then cooled down to the ambient temperature. The authors confirmed that the residual compressive strength of the heated specimens decreased with increasing temperatures and the UPV decreased after the specimens were subjected to temperatures over 400 ºC. Moreover, the results showed that the mixture proportion of concrete does not have a significant influence on the residual strength and UPV ratios of the concrete specimens subjected to elevated temperatures. In addition, the authors proposed relations between the residual strength and UPV ratios for different mixture proportions [4].

The Schmidt hammer test is another non-destructive technique used to estimate the properties (compressive strength and modulus) of concrete at the surface of the structural members. A calibrated hammer measures the rebound of a spring-loaded mass impacting against the surface of the sample. The rebound value can be empirically

correlated with the compressive strength of concrete using a conversion chart provided with the equipment. The results provided by this technique usually present a high scatter and are only representative of a 3 cm layer of concrete [5].

The Fire Behaviour Test (FBTest) [6] is a more recent inspection method, which aims at determining the depth of deteriorated concrete by using water absorption measurements and splitting tensile strength obtained from discs (1,5 cm thick) cut from cores drilled from the structural element subjected to fire. The experimental programme developed by the authors of this method consisted of placing concrete cores into an electric furnace, with only one face exposed directly to the heat. The heating curve was characterised by three linear variations: from ambient temperature to 70 ºC in 10 minutes, from 70 ºC to 170 ºC also in 10 minutes and from 170 ºC to 800 ºC in 30 minutes, and a steady 800 ºC level for 60 minutes. After cooling down to ambient temperature, the discs were cut along the whole length of the core, and the water absorption and splitting tensile tests were performed. The results showed a decrease in the water absorption with the core depth from the face that was directly exposed to heat, until a certain distance (between 4.5 and 6 cm of the heated face); from these depths inwards, the water absorption variation with depth became negligible, suggesting that heat had not affected that part of the concrete. For discs subjected to temperatures above 200 ºC (corresponding to depths lower than 4.5-6 cm), there was an increase of water absorption (relative to the mean value of all the heated cores) with increasing temperatures. Regarding the splitting tensile tests, it was observed that the tensile strength stabilized from depths higher than 6.45 cm, indicating that the inner concrete had not been permanently affected by the heat. The authors concluded that the FBTest is an effective method to estimate the thickness of the fire-damaged concrete; however, its effectiveness has never been tested in structural elements subject to the action of a real fire (with rapid heating) with simultaneous mechanical loading.

In the last three decades, fibre reinforced polymers (FRP) have been used to strengthen/repair different concrete structural elements, due to several advantages they offer (e.g., high strength, non-corrodibility, ease of application) over traditional repair techniques. Jaddoe *et al.* [7] developed an experimental study on heat-damaged RC beams strengthened using near surface mounted (NSM) carbon FRP (CFRP) strips. The beams were heated according to the ISO 834 [8] standard fire curve up 600 ºC and 700 ºC; the maximum temperatures were maintained for 2 h and then the beams were cooled down to room temperature. The beams exposed to a maximum temperature of 700 ºC were repaired with NSM-CFRP strips embedded in epoxy or cement-based adhesives; flexural tests were then performed at room temperature. The results showed that the beams repaired with NSM-CFRP strips using epoxy and cement-based adhesive increased their load capacity by 34% and 19%, respectively (compared with the heat-damaged beam), with a significant stiffness increase. Regarding the failure modes, it was observed that as the load approached the ultimate capacity of the beams, concrete cover separation started at the cut-off point of the strips and propagated to the middle of the beams, followed by compressive failure of concrete.

In this context, this paper presents the results of an experimental campaign, developed within the author's master dissertation, in which the following main objectives were defined: (i) to assess both field and laboratory inspection techniques applied to fire-damaged RC slabs, and (ii) to investigate the bending behaviour of fire-damaged RC slabs repaired and strengthened with NSM-CFRP strips. To this end, simply supported RC slabs were simultaneously subjected to the ISO 834 standard fire curve for 60 or 120 minutes and to a service mechanical load. Different concrete inspection tests were performed (visual assessment, ultrasonic pulse velocity test, Schmidt test, and Fire Behavior Test – FBTest) and tensile tests were also performed on steel rebars. In addition, an unheated slab, and two fire-damaged slabs, one unrepaired and the other CFRP-strengthened, were subjected to flexural tests at room temperature, with the aim of measuring the effect of the fire-damage and of the efficacy of the NSM-CFRP strips, respectively.

2. Experimental programme

2.1. Test programme

To achieve the aforementioned objectives, different inspection tests were carried out on fire-damaged RC slab strips and flexural tests were performed at ambient temperature on the following six slab specimens (cf. Table 1): one reference slab (unheated – *Ref T20*); one slab exposed to fire for 60 minutes, unrepaired (*Ref Fire*); two slabs exposed to fire for 60 minutes, whose fire damage was assessed with different inspection tests (*Fire 60 - 1* and *Fire 60 - 2*); one slab exposed to fire for 120 minutes that was also assessed (w.r.t. fire damage) with the same inspection tests used in the previous slabs (*Fire 120 - 3*); one slab exposed to fire for 60 minutes, then repaired with NSM CFRP strips (*Fire 60 - R*) and finally subjected to flexural tests at room temperature.

Table 1 - Slab specimens.

Nomenclature	Description
Ref T20	Normal temperature control slab
Ref Fire	Exposed to fire for 60 minutes, unrepaired
Fire 60 - 1	Exposed to fire for 60 minutes, unrepaired, for inspection techniques
Fire 60 - 2	Exposed to fire for 60 minutes, unrepaired, for inspection techniques
Fire 120 - 3	Exposed to fire for 120 minutes, unrepaired, for inspection techniques
Fire 60 - R	Exposed to fire for 60 minutes, repaired with NSM CFRP strips

2.2. Materials

Concrete class C25/30 with cement type CEM II/A-L 42.5R and limestone aggregates was used. Compressive and splitting tensile strength tests were performed according to NP EN 12390-3 [9] and NP EN 12390-6 [10], respectively, at the age of the fire tests (485 days), providing the following average values: compressive strength of 58.2 MPa and splitting tensile strength of 2.8 MPa. The Young's modulus

was estimated as 33.6 GPa, according to Eurocode 2 [11]. During the first 50 days of age, the concrete cylinders and cubes were subjected to different curing conditions than the slabs; the former were kept in a controlled environmental chamber (20 ºC of temperature and 100% of relative humidity), while the slabs were kept at the lab's facilities during the whole period (at room temperature and relative humidity, not controlled).

Steel rebars type A500 were used for all the slabs, and their mechanical properties were determined from tensile tests according to EN 10002-1 [12]. The yield stress, tensile strength and Young's modulus of the 10 mm diameter steel rebars were found to be 569 MPa, 662 MPa and 198 GPa, respectively. The yield and ultimate strains were determined as 4.87‰ and 56.16‰, respectively.

2.3. Geometry of the slab strips

The slab strips tested were 0.25 m wide, 0.11 m thick and 1.50 m long. The internal reinforcement consisted of 3 longitudinal rebars with 10 mm and 6 mm of diameter, respectively, for the lower and upper layers. In the transverse direction, steel reinforcement with 6 mm of diameter and 16 cm of spacing was also applied. Fig. 1 illustrates the reinforcement scheme adopted in all slabs.

2.4. Fire exposure test

2.4.1. Test setup

Fig. 2 illustrates a scheme of the test setup used in the fire exposure tests. The slabs were placed on top of a furnace, being simply supported in a 1.40 m span with two supports (sliding support - SS and fixed support - FS). Both supports were placed on top of steel plates, connected to a steel reaction frame with steel rods. Concrete weights were suspended at both extremities of a load transmission beam, applying two concentrated loads on the slabs' top surface (loads spacing corresponding to thirds of the span). All slab strips were thermally insulated on their lateral faces through an insulation system (ceramic wool) in order to cover the remaining area of the top of the furnace and thereby preventing the heat from escaping.

The tests were performed in an intermediate scale furnace fuelled by propane gas, with 6 burners (3 in each wall) and walls lined with ceramic wool. Although the furnace has a top area of 0.95 m x 0.80 m, the fire was applied to the bottom surface of the slabs on a length of 1.10 m, while both 0.20 m slab's extremities remained thermally insulated. The mechanical load to be applied during the fire exposure was calculated according to the expression (2.4) of the Eurocode 2 [13], resulting in a total load of 17.7 kN.

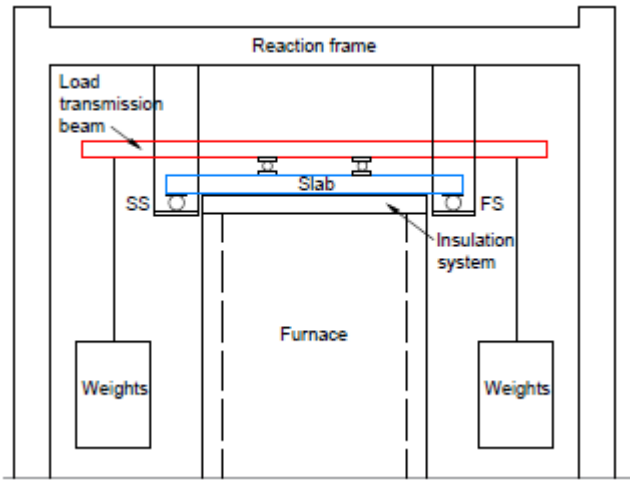

Fig. 2 - Fire exposure tests setup.

2.4.2. Instrumentation and test procedure

The slabs exposed to fire were instrumented with eight 0.25 mm diameter type K thermocouples, in order to measure the temperature in different locations (in concrete and also in steel bars), as shown in Fig. 3. In addition, one thermocouple (*Tair*) was placed above the slab's unexposed (top) surface, in order to measure the air temperature. During the tests, the midspan displacement was also monitored with a *TML DP500-E* wire transducer (500 mm of stroke).

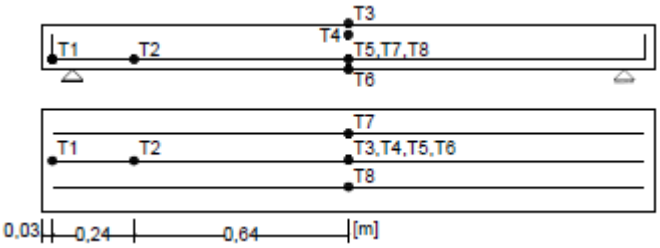

Fig. 3 - Distribution of thermocouples used in the slabs exposed to fire.

The fire exposure tests consisted of two phases: (i) before being exposed to fire, each slab was first subjected to the mechanical load, which was kept constant until the end of the test; this stage ended when the displacement stabilized (about 10 minutes after loading); and (ii) the slab was then exposed to the ISO 834 standard time-temperature curve [8], for 60 or 120 minutes. Finally, the slabs were cooled down to the ambient temperature.

2.5. Inspection techniques

To carry out inspection tests on the fire-exposed slabs, concrete cores were first extracted; the cores were drilled from the slabs exposed to fire, and were also extracted from concrete specimens at room temperature (used as reference). The concrete cores had about 7 cm of diameter, and were taken according to [14]. Some samples were

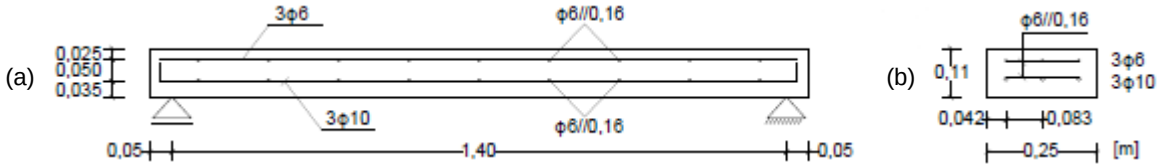

Fig. 1 - Reinforcement distribution: (a) longitudinal view of slabs; (b) cross section of slabs.

cracked, either due to the extraction process itself or due to the concrete degradation caused by the high temperatures and loading; thus, it was not possible to use the same number of samples in all inspection tests. In order to perform the FBTest, discs were sliced along the length of the cores (starting from the face that was directly exposed to fire) with 1 cm of thickness from slab *Fire 60 – 1* and with 2 cm of thickness from the slabs *Fire 60 – 2* and *Fire 60 - 3* and also from the reference core.

2.5.1. Visual inspection

The first phase of visual inspection comprised the observation of the concrete surfaces of the slabs, namely their coloration, microcracking, disintegration or spalling of the concrete cover, as well as the deformation of the element. In a second phase, the cores removed from the slabs were examined; in particular, their coloration, cracking and porosity were observed.

2.5.2. Ultrasonic pulse velocity (UPV) tests

Ultrasonic pulse velocity tests were performed on the whole core specimens and also in the remaining length of specimens, as the discs were sliced from the cores. The UPV was measured according to EN 12504-4 [14], which specifies a minimum specimen length of 150 mm, i.e. above the size of the cores. However, one aimed at assessing the efficacy of this technique when used in smaller samples. The UPV was determined by performing tests on saturated concrete specimens, in which the transmitter and receiver were placed at the top and bottom surfaces of the specimens (direct transmission mode), as illustrated in Fig. 4 (a).

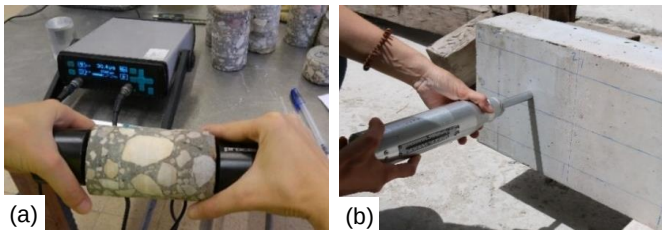

(a) (b)

Fig. 4 - (a) UPV test; (b) Schmidt hammer test applied on the surface of the slab.

2.5.3. Schmidt hammer test

The Schmidt hammer tests were performed according to BS EN 12504-2 [15]. The hammer was used in a horizontal position, perpendicular to the concrete surface tested, as illustrated in Fig. 4 (b). The tests were conducted on the bottom surfaces of the slabs *Fire 60 - 1* and *Fire 120 - 3*, in which 10 measures were taken; and also in the remaining length of core specimens, as the discs were sliced, from sabs *Fire 60 – 2* and *Fire 120 – 3*, and from the reference specimen at room temperature, in which only 5 readings were taken, due to the small sample size (diameter of 7 cm).

2.5.4. Fire Behaviour Test (FBTest)

After the discs had been sliced along the length of the cores, they were kept at 100 ºC in a heated chamber for 24 h, in order to dry. The discs were then cooled down to ambient temperature and weighted, to determine the dry mass (m_{dry}). In the next step the discs were left immersed in water for 48 h, and then they were weighted, to determine the saturated mass (m_{sat}). The saturated discs were finally subjected to splitting tensile tests according to NP EN 12390-6 [10], using an *Instron* universal testing machine, under a constant load rate of 0,05 MPa/s. The water absorption after immersion and the tensile failure stress (f_{ctm}) were evaluated from expressions (1) and (2), respectively, where N_c is the failure load, D is the discs' diameter and e is their thickness.

$$Water\ absorption = \frac{m_{sat} - m_{dry}}{m_{dry}} \times 100\ [\%] \quad (1)$$

$$f_{ctm} = \frac{2 \times N_c}{\pi \times D \times e}\ [MPa] \quad (2)$$

2.5.5. Tensile tests on steel bars

A sample of the steel rebars was extracted from the slab *Fire 120 – 3* (after being exposed to fire) and then it was subjected to a tensile test, according to EN 10002-1 [12]. Its properties were compared with a reference rebar extracted from the slab *Ref T20*.

2.6. Repair of slab *Fire 60 - R*

Slab *Fire 60 – R*, after being subjected to fire for 60 minutes, was repaired with NSM CFRP strips embedded in epoxy adhesive. The following section describes the materials and procedure adopted in this repair/strengthening technique.

2.6.1. Materials

The CFRP strips used in this study (*S&P Laminates CFK 150/2000*) were 1200 mm long, 10 mm wide and 1.4 mm thick (with a 14 mm^2 cross sectional area). Previous studies carried out at IST [16] provided the following average properties: tensile strength of 2850 MPa, elastic modulus of 168 GPa and ultimate strain of 16‰. The effective strain was 7.84‰, determined according to expression (7) of [17]. The CFRP strips were bonded to concrete using a two-component epoxy adhesive (*S&P Resin 220*).

2.6.2. Repair technique

The NSM-strengthening system was installed in the slab soffit according to the following procedure: two slits (5 mm wide, 15 mm deep, 77 mm of spacing) were made on the concrete surface using a diamond blade cutter; the slits were cleaned with compressed air and then filled with adhesive; the strips were manually introduced into the slits and the adhesive in excess was removed. Before the CFRP strips were inserted into the slits, two *TML* electrical strain gauges (model *FLK-6-11-3L*) were installed at their midspan section.

2.7. Flexural tests at room temperature

The flexural tests were performed in a four-point simply supported configuration, with two concentrated loads applied at thirds of the 1.40 m span. Regarding the instrumentation, an electrical *TML* displacement transducer (model *CDP-100*, 100 mm of stroke) was used at midspan to measure the vertical deflection of the slabs. A *Novatech* load cell (200 kN of capacity) was used to measure the applied load. *TML* electrical strain gauges (model *FLK-6-11-3L*) were used to measure the axial strains during the tests, in the longitudinal rebars (upper and lower layers) of slab *Ref T20* and in the CFRP strips of slab *Fire 60 - R*, both at midspan section.

3. Results and discussion

3.1. Thermal and mechanical behaviour

3.1.1. Temperature profiles

The temperature profile obtained during the test of slab *Ref Fire* is presented in Fig. 5; it is worth mentioning that all slabs exposed to fire for 60 minutes had a similar thermal response. The temperature profile of slab *Fire 120 - 3* is presented in Fig. 6.

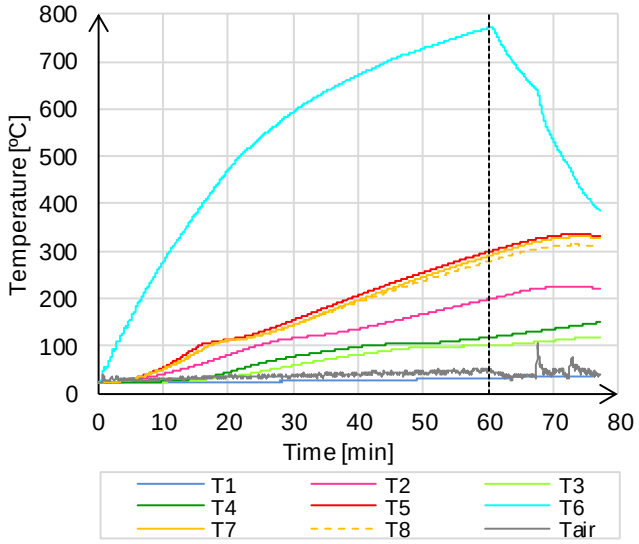

Fig. 5 - Temperature profile of slab *Ref Fire*.

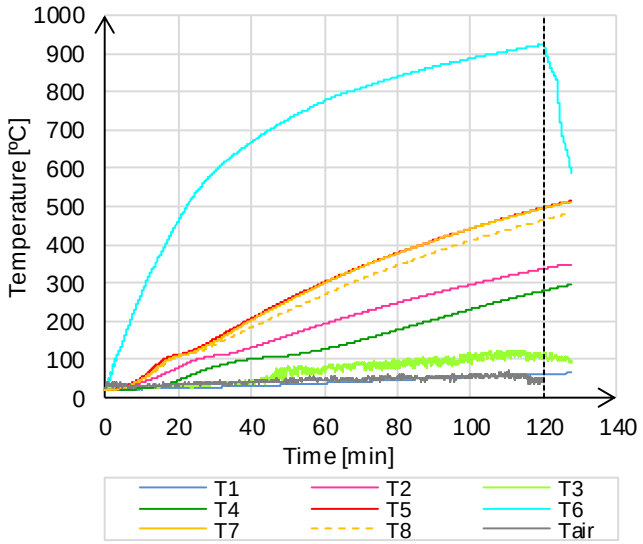

Fig. 6 - Temperature profile of slab *Fire 120 - 3*.

The results showed in both figures are in agreement with the expected ones and validate the readings obtained: (i) the temperature values decreased from the bottom face of the slabs (directly exposed to fire, thermocouple T6) to the top part of the section (thermocouple T3); (ii) there was a progressive increase of the temperatures with the fire exposure time in all thermocouples, although at different rates; (iii) the temperature values in thermocouples T6 followed closely the ISO 834 standard fire curve; (iv) after the fire exposure time (60 or 120 minutes), the temperature in T6 decreased due to (i) turning-off of the furnace burners and (ii) the removal of the furnace front door and the lateral thermal insulation of the slabs. In all tests it was observed that when the temperature approached 100 ºC (in the most thermocouples, with exception of T1 and T6) the heating rates significantly decreased, increasing a few minutes later; this behaviour is due to the evaporation of the water of the concrete - that occurs at 100 ºC - and that consumes a part of the heat transferred to the slabs until all the water evaporates. The thermocouples T5, T7 and T8 presented very similar temperature profiles, as expected. These results showed that the heat exchanges occurred mainly at the slabs' bottom surface, while those that may have occurred on the side faces were negligible; these results confirmed that the thermal exposure imposed on the tests is characteristic of "slab" elements (heat flux imposed on a single face), as intended. Additionally, thermocouple T1 (located in the unexposed zone) presented a very low temperature increase (maximum of about 60 ºC), with a very low heating rate, which confirmed an adequate insulation in the support zones. Table 2 presents the maximum temperature values attained during the tests.

Table 2 - Maximum temperatures obtained.

Maximum temperature values (ºC)	60 min. slabs	120 min. slab
Furnace	947	1048
Slabs' bottom surface - T6	773	925
Steel reinforcement -T5, T7, T8	338	514
Slabs' upper surface - T3	119	124

3.1.2. Mechanical behaviour

The midspan displacement increase (measured in the second phase of the tests) obtained during the fire exposure tests is presented in Fig. 7.

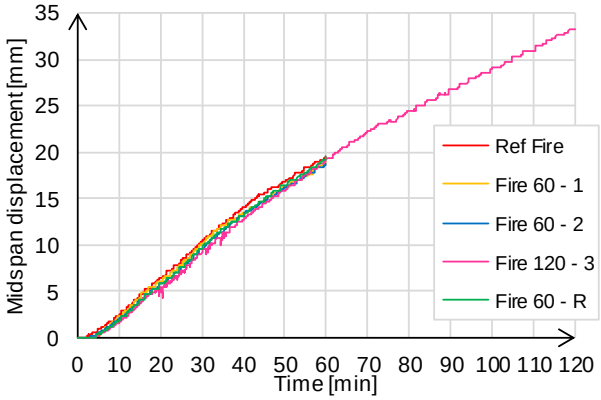

Fig. 7 –Midspan displacement increase *vs.* time of fire exposure.

Regarding the mechanical response during the fire exposure tests, it was found that the variation of midspan displacement of all the slabs increased with the time of fire exposure at an approximately constant rate; this expected behaviour was due to the stiffness (and strength) decrease of the constituent materials. At the end of the tests, the midspan displacement increased 19 mm and 33 mm in the slabs exposed to fire for 60 and 120 min, respectively.

3.2. Inspection techniques

In the following sections the results of the inspection tests are presented and discussed.

3.2.1. Visual inspection

3.2.1.1. Slabs

After exposure to fire for 60 minutes, the bottom surface of slab Fire 60 – 1 presented a whitish grey colour with some shades in yellowish brown in the central zone (*cf.* Fig. 8); this coloration is in accordance with the literature and the temperatures measured. In Fig. 8 (b) it is possible to notice that the whitish grey colour in the central zone changed to a pink tone in the transition zone, and finally to grey (original concrete colour); the pink coloration corresponds to temperatures between 300 and 600 ºC, which is in accordance with the lower temperature reached in that zone. There was also a colour change in the lateral face of the slabs, being more distinctive in the central zone; thus, as presented in Fig. 8 (a), in the zone between the lower face and up to about half-height, there is a pink tonality, and for higher depths the concrete presents its original colour. The slabs exposed to fire for 60 minutes showed surface cracking at the bottom face, with greater expression in the zone directly exposed to fire.

The slab *Fire 120 – 3* presented more damage in the bottom surface than the slabs exposed to fire for 60 minutes, as expected. Indeed, the slabs exposed to fire for 120 minutes exhibited a more significant permanent deformation (about 37 mm) than the other slabs (in average, 22 mm). In addition, 24 h after the fire exposure test, the concrete cover in the central zone showed disaggregation (*cf*. Fig. 9 (a)), which may be related to the degradation of the cement paste that resulted from its shrinkage during cooling down. Since the concrete cover was completely disaggregated (*cf.* Fig. 9 (b)), it was removed (*cf.* Fig. 9 (c)), which allowed to observe the cement paste and the aggregates. The transition zone (between the exposed and unexposed zones) presented a pink tone and, therefore, it was moderately affected by the thermal action. In addition, a generalized superficial cracking was observed, most likely due to the heating and the differential expansion between the aggregates and the cement matrix.

3.2.1.2. Cores

In the upper face of the cores (corresponding to the lower face of the slab), a yellow-beige colour was observed in the cement paste, and it was possible to verify voids and micro-cracks that, together with the reduction of the mechanical properties, led to a disintegration of part of the cores, especially in the samples removed from the slab *Fire 120 -3*, as illustrated in Fig. 10. In addition, the aggregates and the cement paste presented a pink/red and yellowish discoloration, respectively, this difference being less visible in depth (in relation to the initial coloration).

For both colour changes (aggregate and cement paste), these changes were more expressive and visible in a greater depth in the sample removed from the central zone of the slab exposed to fire for 120 minutes, compared to the samples taken from the slabs exposed to fire for 60 minutes (*cf*. Fig. 10). In both slabs, as expected, there was no change in the concrete colour next to the upper (cold) surfaces. Moreover, in all samples removed from the zone directly exposed to fire, concrete exhibited porosity in a depth of about 3 cm.

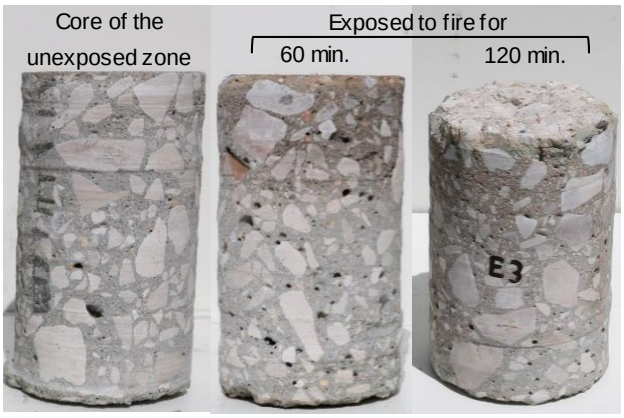

Fig. 10 – Comparison between two samples removed from the central zone of the slabs exposed to fire for 60 and 120 min, and one sample removed from the insulated zone (support).

Fig. 8 – Appearance of slab *Fire 60 – 1* after exposure to fire: (a) Overview of the bottom and lateral surfaces of the slab; (b) Intermediate zone of the bottom surface of the slab, between the exposed zone and the unexposed zone.

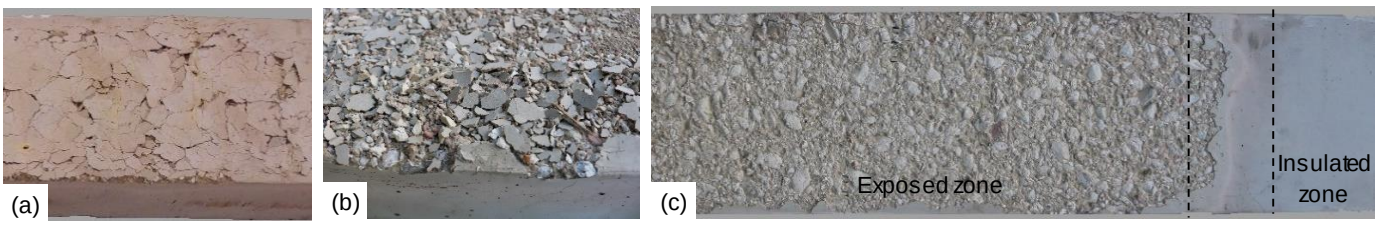

Fig. 9 – Appearance of the bottom surface of the slab *Fire 120 – 3* after exposure to fire: (a) 24 h after; (b) After cooling of the concrete; (c) Final aspect.

3.2.2. Ultrasonic pulse velocity test (UPV)

Fig. 11 presents the residual UPV ratio (relative to the reference UPV, measured in the reference concrete core at ambient temperature) *vs.* the longitudinal distance (relative to one end of the slab), for each of the slabs. The points marked in this figure correspond to the measurement of the UPV in the total height of the concrete cores; it should be noted that only two "complete/intact" cores of slab *Fire 120 – 3* were extracted (located in the unexposed zone), due to the very extensive damage of concrete induced in the central zone of that particular slab.

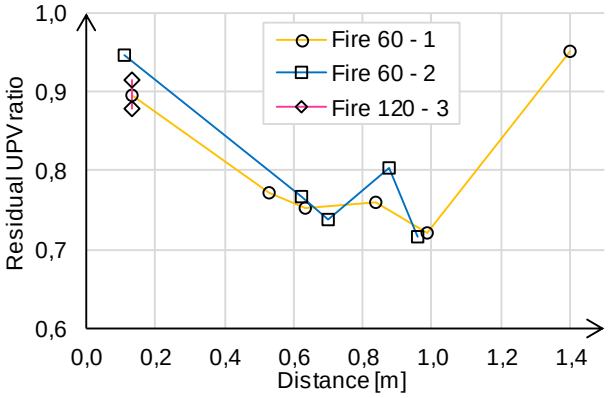

Fig. 11 – Residual UPV ratio *vs.* longitudinal distance.

The cores from the unexposed zones (thermally insulated) showed reductions of the UPV ratio up to 12% (considering the average of the entire depth of the concrete core); these results confirm that the concrete located in the zones not exposed directly to the fire were only slightly affected; this is in agreement with the (relatively low) temperatures measured in those zones. On the other hand, as expected, it was found that the relative UPV values in the zone directly exposed to fire were lower than those obtained from the thermally insulated zones (despite some scatter). Thus, the concrete cores extracted from the central zone of the slabs presented a reduction of the UPV ratio between 20% and 28% (again, considering the average of the entire depth of the concrete core), which confirms, as expected, the higher damage introduced to the concrete that was directly exposed to fire.

The results obtained from the UPV (relative) measured in the remaining length of cores (after successively slicing discs from the original cores), along the slab thickness, are presented in Fig. 12 and Fig. 13 for specimens removed from slabs *Fire 60 – 2* and *Fire 120 – 3*, respectively. In these figures the maximum temperatures (obtained from a numerical model [18]) expected at each depth (in the midspan section) are also presented. With the exception of the curves labelled as A1, F1, E1, all curves presented in these figures were obtained from concrete cores extracted from the central zone of the slabs (directly exposed to fire).

Fig. 12 suggests that, in general, there is no clear relationship between the UPV ratio and the distance to the lower face of the slab. Nevertheless, in cores extracted from the central zone of the slab and measured in their total length (distances near 0 mm) there was a reduction of 20% in the UPV (compared to the reference value). For higher distance values and, consequently, lower temperatures, there was a decrease of the UPV ratio in samples A2 and A3, which was not expected, since the degree of concrete damage should decrease with depth; however, the sample A5 presented a relative increase of the UPV ratio with the increase of the distance to the bottom face of the slab, suggesting a more compact and resistant concrete, as expected. The sample A1 (taken from the extremity) presented higher values of UPV ratio than the cores of the central zone, as expected; however, the UPV ratio of this sample showed reductions along the slab thickness, which is not logical.

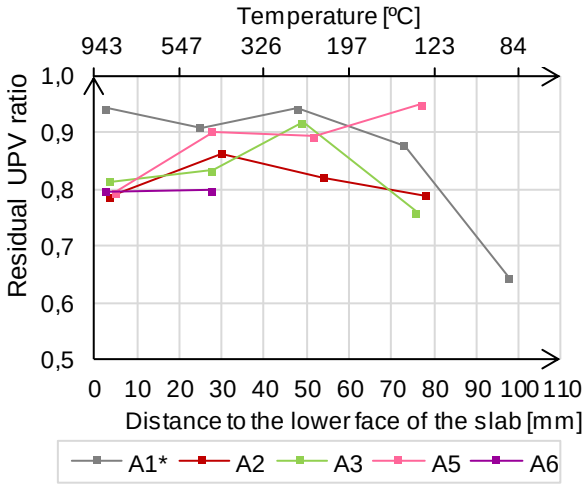

Fig. 12 – Residual UPV ratio *vs.* distance to the bottom face of the slab *Fire 60 - 2*.

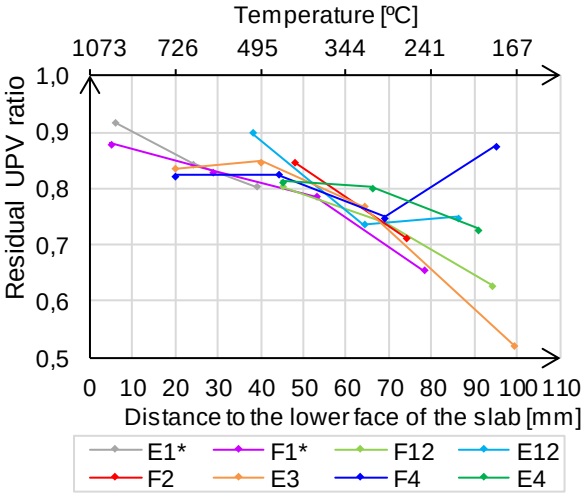

Fig. 13 – Residual UPV ratio *vs.* distance to the bottom face of the slab *Fire 120 - 3*.

The specimens extracted from the slab exposed to fire for 120 minutes showed in general a decreasing trend of the UPV ratio with the increase of the distance to the bottom face of the slab, as presented in Fig. 13 – this was not expected nor it is logical. There was no significant difference in the values and the trend of the UPV ratio between the specimens removed from the insulated zone and the ones taken from the central zone (directly exposed to fire).

Overall, the results obtained with this technique suggest/confirm that this test does not provide reliable results of the actual damage underwent by fire exposed concrete, when applied to concrete samples of reduced thickness and/or in samples with about 7 cm of diameter.

3.2.3. Schmidt hammer test

Fig. 14 presents the rebound number (N) with the corresponding standard deviation, obtained from measurements made on the lower surfaces of the slabs, and the estimated values of the concrete compressive strength, as a function of the longitudinal distance where the tests were carried out.

As expected, the slab *Fire 120 – 3* presented lower rebound number values than those measured on the slab exposed to fire for 60 minutes, since the damage introduced in the first slab was higher. The standard deviation values associated to the measurements in the slab *Fire 120 - 3* were considerably higher than those obtained in the slab *Fire 60 - 1*, which can be justified by the fact that measurements of the rebound number in the central zone of the slab *Fire 120 – 3* were carried out on an irregular surface (in which concrete cover disintegration occurred). Despite the variability of the rebound numbers, from the results presented in Fig. 14 it was possible to conclude that this inspection technique allowed to assess the reduction of the compressive strength of the concrete cover due to fire action, which, as expected, was higher in the slab exposed to fire for 120 min.

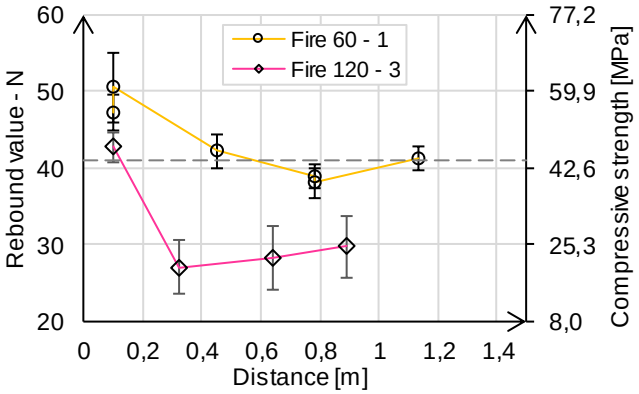

Fig. 14 – Rebound number and the corresponding compressive strength of concrete *vs.* longitudinal distance.

Fig. 15 and Fig. 16 illustrate the residual compressive strength of concrete, for samples extracted from slabs Fire 60 – 2 and Fire 120 – 3, respectively, as function of the distance from the face of the remaining samples (in which the test was performed) to the bottom surface of the respective slab. In those figures the maximum temperature values in the concrete surface, at midspan section, estimated using a numerical model [18] are also presented. All cores presented in the legend of the figures refer to the central zone of the slabs (exposed directly to fire), except for the cores A1, F1, E1.

As predicted, in all the samples tested there was a reduction of the compressive strength of the concrete (compared to the value obtained from the reference core, at room temperature), even in the samples removed from the support zones (cores A1, E1 and F1); this indicates that the concrete in those areas suffered some damage, although not having been exposed directly to fire. The values obtained from the core A1 were higher than those obtained from specimens extracted from the central zone of the slab (*cf.* Fig.15); and the same was found between samples E1 and F1 and the remaining samples of the slab Fire 120 - 3 (*cf.* Fig.16). These results indicate, as expected, that the concrete located in the support zone (thermally insulated) was less affected by the fire action than that of the central zone. In addition, it was possible to verify that the concrete samples that had been directly exposed to fire for 120 minutes presented lower (estimated) compressive strength values than the samples that were exposed to fire for 60 minutes. Concerning the evolution of the concrete strength ratio with the depth at which the samples were tested, it was observed in both slabs that this value tends to decrease as the distance to the lower face of the slab increases; although the scatter in the results obtained is significant, this result was not expected, indicating/confirming that the Schmidt hammer test does not provide sufficiently accurate results of the actual damage underwent by concrete when applied to concrete samples of reduced size (thickness and/or diameter).

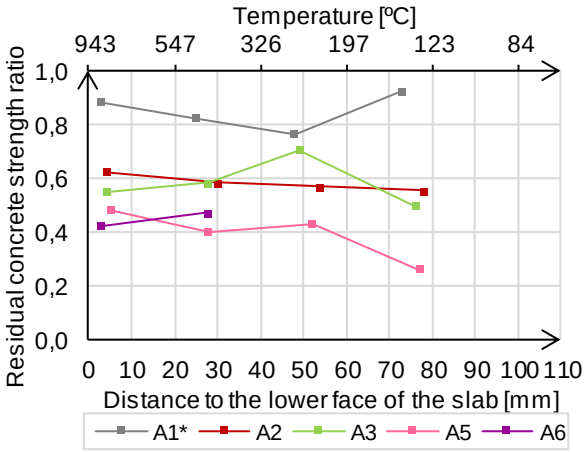

Fig. 15 – Residual concrete strength ratio *vs.* distance to the bottom face of the slab.

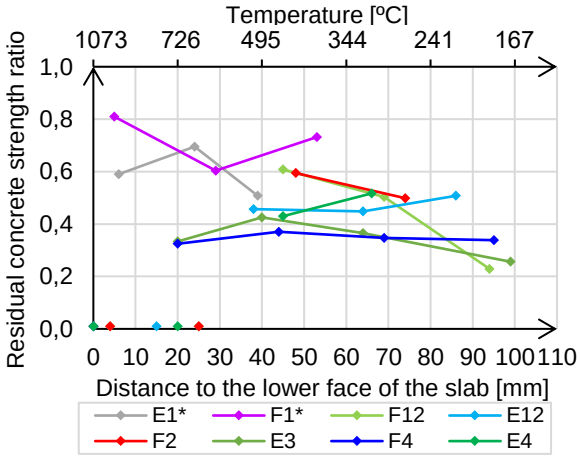

Fig. 16 – Residual concrete strength ratio *vs.* distance to the bottom face of the slab.

3.2.4. Fire Behaviour Test (FBTest)

In the water absorption tests, carried out on discs obtained from slabs exposed to fire for 60 minutes, there was no clear reduction of water absorption after immersion with depth, nor was there any constant level of water absorption values from a certain distance to the bottom face of the slab, unlike the results obtained in the work by Branco *et al*. [6]. In the discs removed from the central zone of the slab exposed to fire for 120 minutes, it was possible to observe a general reduction of the water absorption values with depth, as expected, since

higher values of water absorption are associated to greater porosity and cracking levels (resulting from the fire action). In addition, from a depth between 70 and 80 mm the variation of the water absorption was very small; which indicated that the concrete from these depth inwards was not significantly affected by the heating. From the results obtained in the water absorption tests, Fig. 17 plots the water absorption variation of the samples removed from the central zone of the slabs (compared to the reference value, 3.98%, measured in discs from the reference cores) *vs.* maximum temperature attained in the hottest surface of the disc. The temperatures were estimated from the already mentioned numerical model [18].

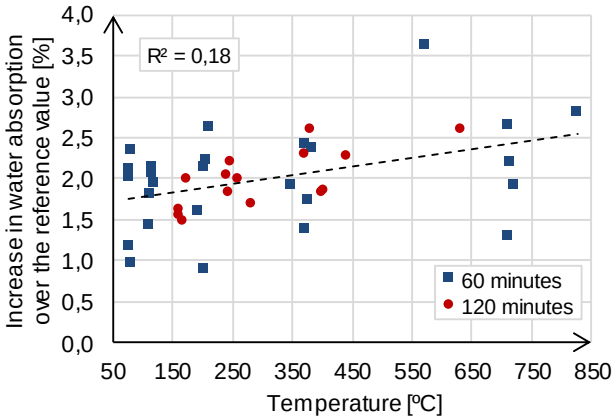

Fig. 17 – Increased in water absorption (over the reference value) *versus* temperature.

From the diagram in Fig. 17 it is possible to observe an increase in the water absorption (relative to the reference value) with the increase of the temperature reached in the concrete discs and, consequently, with the approach to the bottom surface of the slab. However, the linear regression obtained presented a very low coefficient of determination of only 0.18, reflecting the significant scatter of the values obtained. This scatter may be due to the high thermal gradients caused by the exposure to the standard fire curve used in the present study, compared with the (relatively slow) heating curve defined in the FBTest [6], which (in the present study) seems to have led to a greater degree of damage in the discs closer to the bottom surface of the slabs.

From the splitting tensile tests performed on samples taken from the slab exposed to fire for 60 minutes, it was possible to observe, in general, an increase of the tensile strength with the distance (of the discs) to the bottom face of the slab. In addition, in the cores removed from the central zone of the slabs, it was verified that as the distance to the lower face of the slab increases, the tensile strength values approach those obtained for the reference samples. Unlike what was observed on the slab exposed to fire for 60 minutes, the discs obtained from the cores of the central zone of slab *Fire 120 – 3* did not provide consistent tensile failure stress values, although there was an increasing trend of the tensile strength with depth. Based on the results of the splitting tensile tests, a diagram with the variation of the tensile failure stress (below the reference value of 3.05 MPa) *vs.* temperature of the samples removed from the central zone of the slabs was built (Fig. 18).

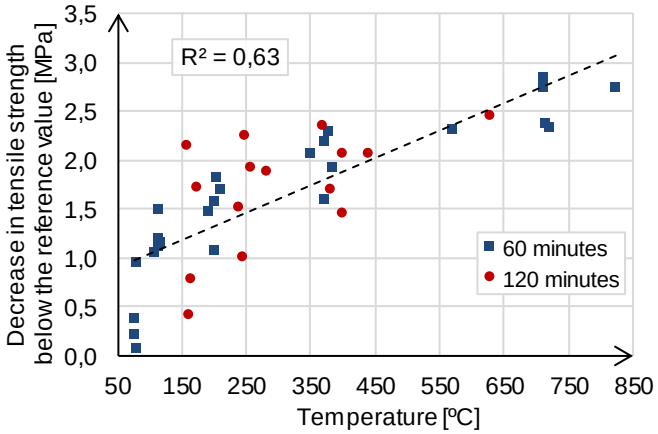

Fig. 18 – Decrease in tensile failure stress (below the reference value) *versus* temperature.

By analysing Fig. 18, it can be concluded that the higher the temperature reached, the higher is the reduction in the splitting tensile strength relative to the reference value. In addition, there was now an acceptable correlation between these two variables, with the linear regression determined presenting a coefficient of determination of 0.63.

The FBTest carried out in the present experimental campaign did not allow to clearly identify the thickness of concrete damaged by fire. However, it was possible to conclude that the splitting tensile test provides more conclusive results than the water absorption test with respect to the degradation of the properties of concrete subjected to elevated temperatures. It should be noted that the concrete samples tested in the present study were subjected to the standard fire curve and, simultaneously, to a mechanical loading, which may have led to a greater degradation of the residual properties of concrete compared to the procedure adopted by the authors who originally presented the FBTest method (relatively slow heating without mechanical loading); even so, this method allowed to quantify the residual tensile strength of concrete as a function of the maximum temperature attained.

3.2.5. Tensile tests on steel bars

The results of the tensile test on the steel bar removed from the slab *Fire 120 – 3* are presented in Table 3. It is possible to conclude that the steel rebar was not significantly affected by the elevated temperatures, with the yield stress (f_{sy}) and the Young's modulus (E_s) remaining practically unchanged (variations below 2%). This could be justified by the fact that during the tests the steel rebar was subjected to a maximum measured temperature less than 514 ºC and/or by a possible recovery of part of the stiffness/resistance after cooling. The tensile strength (f_{su}) of the steel rebar also remained unchanged and the ductility ($\varepsilon_{su}/\varepsilon_{sy}$) increased significantly after exposure to elevated temperatures.

Table 3 – Results of the tensile test on steel rebars

Slab	f_{sy} (MPa)	f_{su} (MPa)	E_s (GPa)	ε_{sy} (‰)	ε_{su} (‰)	ε_{su} / ε_{sy}
Ref T20	569	662	198	4,87	56,16	11,53
Fire 120 - 3	582 (2%)	663 (0%)	200 (1%)	4,92 (1%)	95,95 (71%)	19,50 (69%)

3.3. Flexural test at room temperature

3.3.1. Load-deflection behaviour

The load *vs*. midspan displacement curves of the three slabs tested are presented in Fig. 19. It is worth mentioning that it was not possible to obtain results from the flexural test performed on the reference slab, due to a problem in the instrumentation; thus, the curve of slab *Ref T20* presented was obtained from a flexural test at room temperature carried out in another thesis (Santos [18]), on a similar slab.

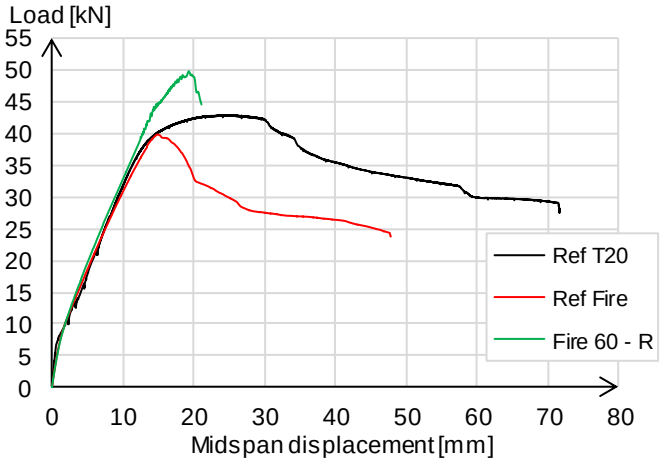

Fig. 19 – Load-midspan displacement curves, flexural tests.

Up to a load of 7 kN, slab *Ref T20* presented the highest stiffness corresponding to the elastic phase, until the beginning of cracking. As the load increased, there was a gradual stiffness decrease due to cracking; for loads above 32 kN a significant decrease in stiffness (and force) was observed, associated with a high deformation, corresponding to the yielding of the (tension) steel reinforcement. In a first phase, up to a load of 8 kN, the slab *Ref Fire* showed a stiffness slightly lower than that observed in slab *Ref T20*, as the slab was already cracked due to the thermal and mechanical actions. For higher loads, slab *Ref Fire* presented approximately constant stiffness up to the peak load, although the slope of the F-d gradually decreased when the peak load was approaching. However, there were no significant reductions in strength at failure and stiffness (reductions of about 7% and 8%, respectively), although the displacement associated to the peak load decreased significantly (-41%). The relatively small reductions in strength and stiffness are due to the fact that the mechanical properties of the steel reinforcement were not affected by fire (as concluded in section 3.2.5); moreover, the compressive strength of concrete on the slabs' upper face was not significantly reduced, which also contributed to a good flexural behaviour of this slab. Regarding the slab *Fire 60 - R*, it was found that the repair/strengthening with CFRP NSM strips was responsible for the increase of load carrying capacity by 16%, although the stiffness remained practically unchanged (increased 1%). In a first phase, up to 8 kN, the F-d curve presented a similar slope to that of slab *Ref Fire*; after which the stiffness decreased due to concrete cracking; for load values higher than 44 kN, a significant reduction of stiffness was observed until failure occurred.

3.3.2. Failure modes

The slabs *Ref T20* and *Ref Fire* (*cf.* Fig. 20) failed due to concrete crushing in the compression zone, with yielding of steel rebars, as it was expected. The slab *Fire 60 – R* failed due to shear failure, with a good bond between the CFRP strips, the epoxy adhesive and the surrounding concrete being observed, thus highlighting the effectiveness of the flexural strengthening technique (*cf*. Fig. 21).

Fig. 20 – Failure mode of slab *Ref Fire*.

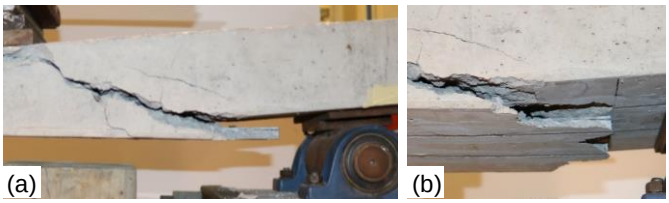

Fig. 21 – Failure mode of slab Fire 60 – R: (a) general view; (b) detail of the bottom face of the slab.

5. Conclusions

From the results obtained, the following main conclusions can be drawn:

1. The application of the UPV and *Schmidt* tests at different depths did not provide reliable results, suggesting/confirming that these methods do not provide sufficiently accurate results (*i.e*. representative of the actual fire damage underwent by concrete) when applied to concrete samples of reduced size.

2. The splitting tensile test (carried out within the FBTest) provided more conclusive results about the degradation of the concrete properties subjected to elevated temperatures compared to the water absorption test.

3. The flexural stiffness and load capacity of the slab exposed to the ISO 834 fire for 60 minutes were only slightly affected by the fire; this was mainly due to the fact that the steel reinforcing bars were not affected by the elevated temperatures neither the concrete in the upper part of the slab.

4. The load capacity of the slab repaired with NSM CFRP strips increased up to 16% (compared with the unheated slab), as expected. However, the repair technique did not allow to take full advantage of the ductility of the steel reinforcing bars, due to the occurrence of premature (and brittle) shear failure. Moreover, and also as expected, the repaired slab did not present a significant increase of stiffness.

5. Nevertheless, the present study confirmed that applying NSM CFRP strips with epoxy adhesive to repair fire damaged RC slabs is a promising method to restore their flexural capacity.

6. References

[1] I. A. Fletcher, S. Welch, J. Torero, R. O. Carvel, A. Usmani, “Behaviour of concrete structures in fire”, *Thermal Science,* vol. 11, nº 2, pp. 37-52, 2007.

[2] B. Erlin, W. G. Hime, W. H. Kuenning, “Evaluation fire damage to concrete structures”, *Concrete Construction,* vol. 17, nº 4, 1972.

[3] J. P. C. Rodrigues, A. J. M. Correia, “Técnicas de avaliação das propriedades mecânicas residuais do betão após incêndio”, em *SIABE - Simpósito Ibero-Americano*, Julho, 2005.

[4] H. Yang, Y. Lin, C. Hsiao, J. Liu, “Evaluating residual compressive strength of concrete at elevated temperatures using ultrasonic pulse velocity”, *Fire Safety Journal,* vol. 44, nº 1, pp. 121-130, 2009.

[5] E. N. B. S. Júlio, “Avaliação "in situ" da resistência à compressão do betão”, em *2º Seminário - A Intervenção no Património. Práticas de Conservação e Reabilitação*, Faculdade de Engenharia da Universidade do Porto, Outubro, 2005.

[6] J. R. Santos, F. A. Branco, J. Brito, “Assessment of concrete structures subjected to fire - the FBTest”, *Magazine of Concrete Research,* vol. 54, nº 3, pp. 203-208, 2002.

[7] A. Jadooe, R. Al-Mahaidi, K. Abdouka, “Experimental and numerical study of strengthening of heat-damaged RC beams using NSM CFRP strips”, *Construction and Building Materials,* vol. 154, pp. 899-913, 2017.

[8] ISO 834, “Fire resistance tests. Elements of building construction”, International Standards Organization, 1975.

[9] NP EN 12390-3, "Testing hardened concrete, Part 3: Compressive strength of test specimens", IPQ, 2009.

[10] NP EN 12390-6, “Testing hardened concrete, Part 6: Tensile splitting strength of test specimens”, IPQ, 2003.

[11] NP EN 1992-1-1, “Design of concrete structures - Part 1-1: General rules and rules for buildings”, IPQ, 2010.

[12] EN 10002-1, “Metallic materials - Tensile testing - Part 1: Method of test at ambient temperature”, CEN, 2001.

[13] NP EN 1992 1-2, “Design concrete structures, Part 1-2: general rules - Strucutural fire design”, IPQ, 2010.

[14] EN 12504-4, “Testing Concrete, Part 4: Determination of ultrasonic pulse velocity”, CEN, 2004.

[15] BS EN 12504-2, “Testing concrete in structures, Part 2: Non-destructive testing - determination of rebound number”, British Standards Institution, 2012.

[16] J. P. Firmo, “Fire behaviour of reinforced concrete structures strengthned with CFRP strips”, Tese para obtenção do Grau de Doutor em Engenharia Civil, Instituto Superior Técnico, Universidade de Lisboa, 2015.

[17] J. A. O. Barros, S. J. E. Dias e J. L. T. Lima, “Efficacy of CFRP-based techniques for the flexural and shear strengthening of concrete beams”, *Cement & Concrete Composites,* vol. 29, nº 3, pp. 203-217, 2007.

[18] C. Churro, “Simulação numérica do comportamento ao fogo de elementos de betão reforçados com varões em compósito de GFRP”, Dissertação para obtenção do Grau de Mestre em Engenharia Civil, Instituto Superior Técnico, Universidade de Lisboa, Outubro de 2017.

[19] P. R. C. Santos, “Resistência ao fogo de lajes de betão armadas com varões em compósito de GFRP”, Dissertação para obtenção do Grau de Metre em Engenharia Civil, Instituto Superior Técnico, Universidade de Lisboa, Novembro 2016.